

Enhancement of Electrochemical Oxidation of Phenol in Aqueous Solutions Using Polyaniline Coated Graphite Electrode

A.A. Al-Zahrani¹, A.H. El-Shazly², M.A. Daous¹, S.S. Al-Shahrani¹

¹ Chemical and Materials Engineering Department, Faculty of Engineering, King Abdulaziz University, Jeddah, Saudi Arabia.

² Chemical and Petrochemicals Engineering Department, Egypt-Japan University of Science and Technology, New Borg Elarab City, Alexandria, Egypt.

*E-mail: ssaalshahrani@kau.edu.sa

Received: 8 December 2016 / Accepted: 23 May 2017 / Published: 12 July 2017

This work investigates polyaniline coated graphite electrode (PCGE) for the electrochemical oxidation of phenol in aqueous solution. The influences of current density, supporting electrolyte (NaCl) concentration, phenol concentration and electrolysis time removal were investigated. The results showed that the removal efficiency of phenol increased with increasing the current density and NaCl concentration, whereas it was contrariwise related with initial concentration of phenol. It was detected that phenol and its byproducts were rapidly broken down in the presence of chloride ions. Galvanostatic technique was used for building the polyaniline layer over the graphite electrode surface. According to the results, PCGE was an efficient electrode for the electrooxidation of phenol as 35% improvement of PCGE over bare graphite (BG) electrode was achieved. 27.5 kWh/m³ was required for 98% reduction in phenol concentration.

Keywords: electrooxidation, phenols, polyaniline, graphite electrode, wastewater treatment.

1. INTRODUCTION

Conducting polymers especially Polyaniline and polypyrrole have been proved and tested as active electrode materials in many applications in fuel cells [1-3]. Polymer modified electrodes such as polyaniline coated graphite have been shown to be good catalysts [4-7]. Different studies confirm the stability of polyaniline films in different applications such as corrosion resistance [8-11], super capacitors and fuel cells [12]. Patil [13] concluded that the composite electrode of polyaniline and activated carbon have positive synergistic effect between the two materials as they have high energy density and high specific capacitance. Ma and co-authors [14] concluded that the polyaniline (PANI)-promoted Pd catalysts is superior than Pd alone as a catalyst for the electrooxidation of formic acid.

They attributed this to the electronic effect between Pd nanoparticles and polyaniline. Others [15] found that conducting polyaniline films might be convenient substrate for the electrooxidation of ethylene glycol. In another study [16], the authors found that the thickness of polyaniline layer on the platinum doped polyaniline electrodes has influenced the rate of direct methanol oxidation reaction. On the other hand several processes and techniques have been suggested and made for the degradation of phenol and/or its derivatives such as photochemical reactions [17,18], ultrasonic reactions [19], activated carbon adsorption [20]. Electrochemical oxidation (EO) is the most communal electrochemical process for phenol degradation in which the phenol is expected to be broken or oxidized and altered into simpler forms like carbon dioxide and water[21]. The electrochemical oxidation of phenols to CO₂ happens through complex mechanisms that contain several steps including transport of the organic compound to the electrode surface, followed by adsorption, electron transfer and surface reaction with hydroxyl radicals, produced from breakdown of water leading to mineralization of the organic compound [22,23]. This research investigates the application of polymer-modified graphite electrode PCGE for the electrooxidation of phenol under different operating conditions.

2. EXPERIMENTAL WORK

2.1. Preparation of polyaniline coated graphite anode

Electrochemical polymerization of aniline was carried out in one-compartment cell. The working electrode was made of graphite rod, while the counter and reference electrodes were made of silver sheet and Ag/AgCl respectively. The reaction conditions were fixed at 0.1M aniline, 0.5M oxalic acid, 5mA/cm², pH= 1.5 and 20 minutes reaction time. Finally, the PCGE was washed with purified water and dried.

2.2 Electrochemical oxidation experiment

Electrochemical experiments were carried out using an experimental device potentiostat. All the experiments were performed by galvanostatic technique. The voltammetric curves were measured at 25°C using the three-electrode cell: each of the three kinds of electrode at a time, of PCGE as working electrode, Ag/AgCl as a reference electrode, and silver sheet as counter electrode. Supporting electrolyte as NaCl was used for the purpose of producing hypochloride ions that will be responsible for phenol oxidation reaction. Phenol concentration before and after treatment measuring by UV Spectroscopy. The phenol removal percentage was calculated using equation 1:

$$\% \text{Removal} = (C_o - C_t) / C_o \quad (1)$$

where C_o and C_t are the initial concentrations of phenol and the phenol concentrations (mg l⁻¹) at time t (min) respectively. Also the percentage improvement using the new electrode for the removal

of phenol using the PCGE compared to bare graphite (BG) electrode was calculated using the equation 2:

$$\% \text{ Improvement} = (R_{PCGE} - R_{BG}) / R_{BG} \quad (2)$$

Where R_{PCGE} and R_{BG} are the % removal of phenol using PCGE and % removal of phenol using BG electrode respectively. The XRD, FT-IR spectra of the samples were taken using a spectrometer (Vertex 70, Bruker). and scanning electron microscope (SEM) of polyaniline layer were performed before and after electrooxidation.

3. RESULTS AND DISCUSSION

3.1 Characterization of the PCGE new electrode

3.1.1: FT-IR analysis

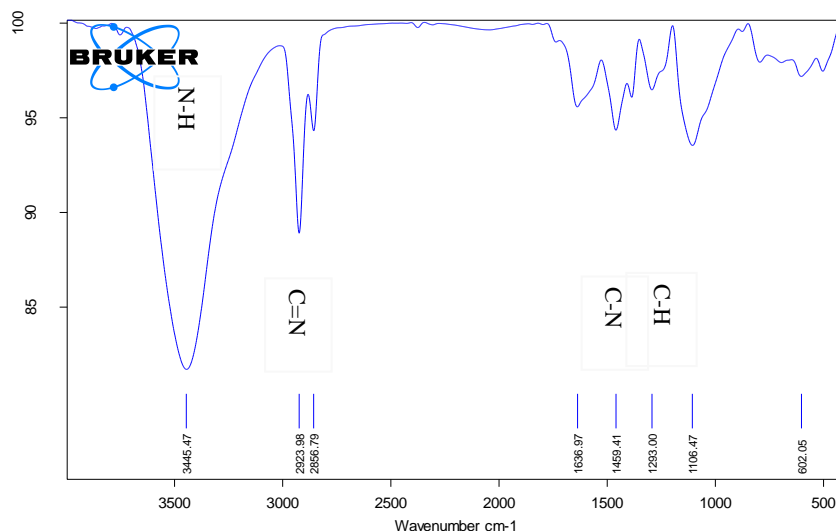


Figure 1. Fourier transform Infrared spectrum of PCGE anode formed at 25°C, 0.1M Aniline, 0.5M Oxalic Acid, Cd=5mA/cm² and 20min.

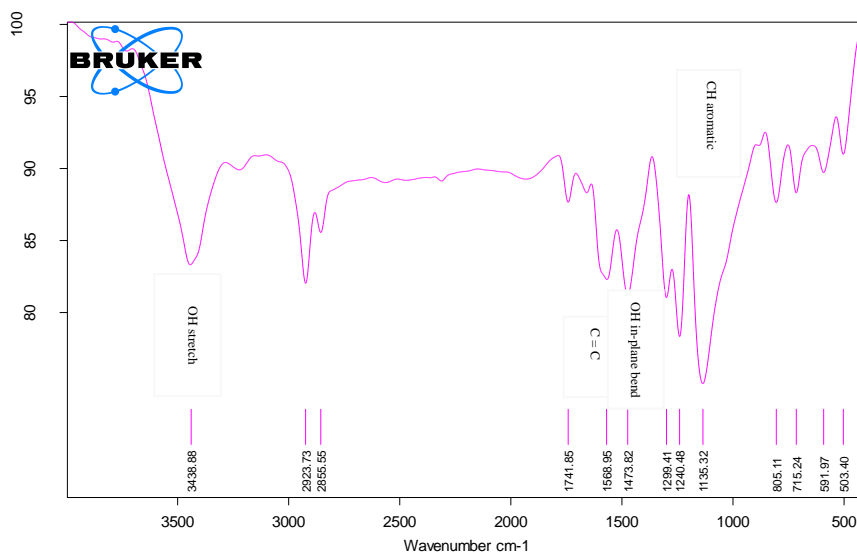


Figure 2. Fourier transform Infrared spectrum of PCGE after phenol degradation carried at 25°C, C₀=10ppm, current density=25mA/cm², 3% NaCl and 60min.

Fig.1 shows FTIR spectra of polyaniline coated graphite anode (PCGE) prepared at conditions, 0.1M Aniline, 0.5M oxalic acid, current density (Cd) = 5mA/cm² and 20min. The characteristic absorption bands thus obtained are 3445.47 for N-H stretching, 2923.98 C=N stretching in aromatic compounds, 1459.41 C-N stretching of primary aromatic amines, 1293 C-H bending vibrations and below 1000 mono substituted benzene. These values were also compared with standards [24] and were found in good agreement. Assignment of the characteristic peaks of PCGE anode after phenol degradation was done using the previously collected spectra of both reactants in aqueous solution. In Figure 2 a typical IR spectrum of a PCGE anode after electrooxidation is also represented.

The appearance of new peak at 3438 cm⁻¹ indicates the OH from the phenol, the peaks at 1588 and 1473 cm⁻¹ show the C=C for aromatic compounds while that at 1135 shows the C-H for aromatic compounds. In addition the new set of peaks at the region from 805 to 503 cm⁻¹ show the asymmetric stretch of phenolic compounds at the surface of the PCGE. The presence of such groups on the anode surface ascribed to precipitation on anode surface due to adsorption and/or ion exchange phenomena during phenol degradation. These results show that adsorption, degradation and ion exchange as well all together might be considered as a proposed mechanism for the phenol removal from wastewater by using the PCGE.

3.1.2. XRD analysis

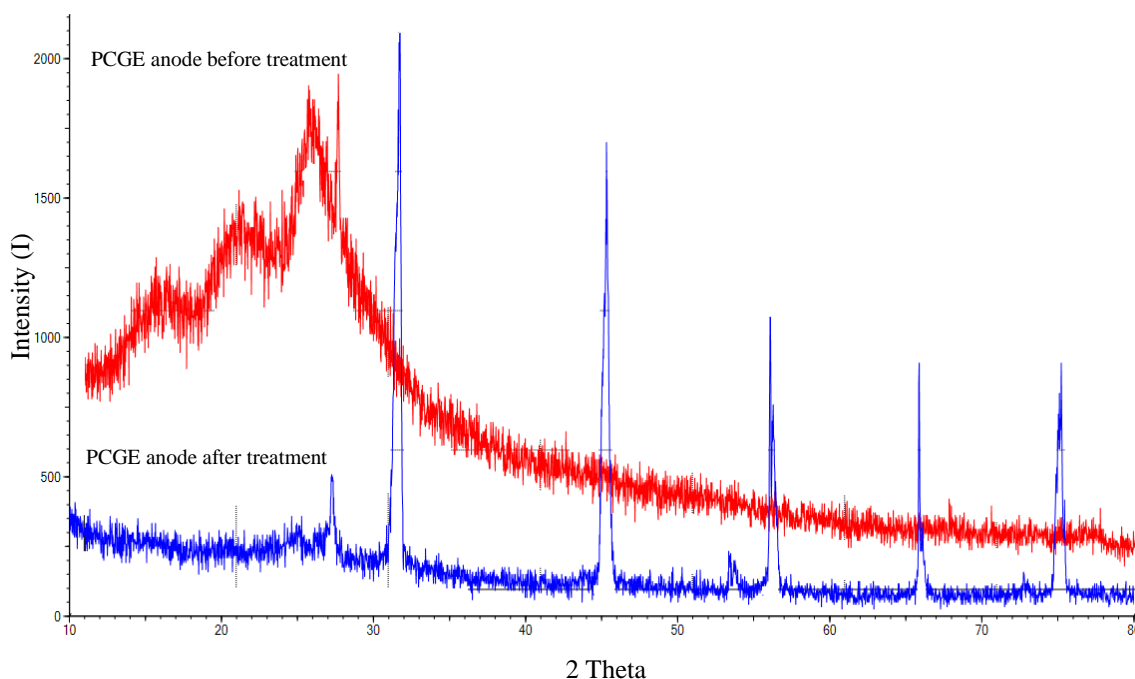


Figure 3. XRD of PCGE anode (a) formed at 25°C, 0.1M Aniline, 0.5M Oxalic Acid, Cd=5mA/cm² and 20min before phenol degradation (b) After phenol degradation.

The XRD data as shown in Fig.3 indicates that new crystalline order has been developed into the structure by the new peaks. Compared with PCGE anode after electrooxidation process, the

obvious characteristic peaks in PCGE can be ascribed to the formation of crystal appearing on the outer layers of anode. XRD analysis of the produced sample was examined using Cu-K radiation which shows two major peaks in the region 2θ from 32-75.

3.1.3. SEM Analysis

The SEM images of PCGE anode before and after electrochemical oxidation of phenol are shown in Fig.4. The results show that two new different layers were present at the surface of the PCGE anode after phenol electro-oxidation. The chemical composition of these layers might be considered as polyaniline and phenol and/or its degradation compounds as well. Moreover, comparing the two SEM images, it was evident that the PCGE anode before phenol degradation characterized by its high porosity compared with that after phenol degradation. These results give prediction about the possibility of adsorption and/or ion exchange mechanisms onto the surface of PCGE anode as possible mechanisms for phenol removal from the waste solution.

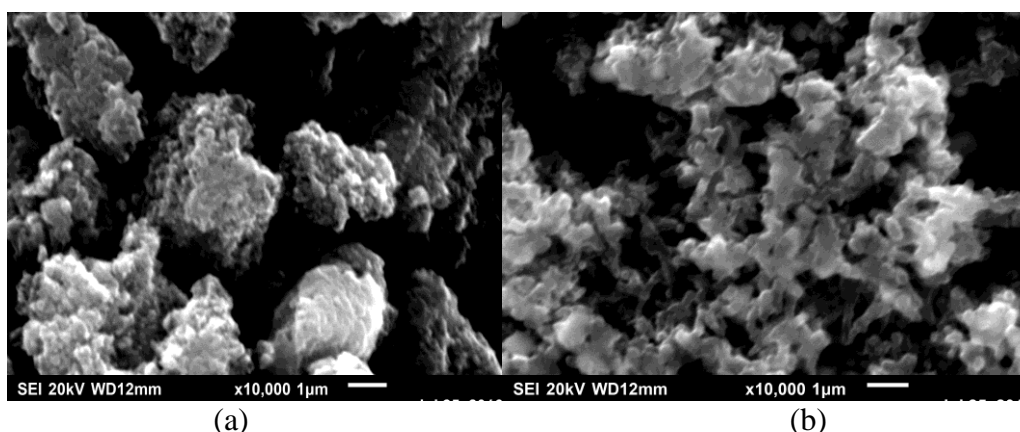


Figure 4. SEM of PCGE anode a) Before treatment and b) After phenol degradation.

3.2. Effect of current density on the electrooxidation of phenol

Fig.5 shows that the effect of current density on phenol removal efficiency with a constant time of 60min. In this research, nominated range of applied current density was from 5 to 25 mA/cm² and selected optimal value of current density was 25 mA/cm² for which 97.85% removal efficiency has been reached within the 60 min. In addition the results show that the oxidation rate was increased by increasing the current density which might be ascribed to the increase in rate of the reaction with increasing the applied current according to the general equation for the rate of mass transfer which may be expressed by the relation[25]:

$$N_D = \frac{i(1-\alpha)}{zF} \quad (3)$$

Where N_D is the mass transfer rate due to diffusion, I is the current, α is the ionic transference number, z and F are the ionic valence charge and the Faraday's constant (amp. s/g. equivalent) respectively. Furthermore, bubble generation rate at the cathode increases and the bubble size decreases with increasing current density.

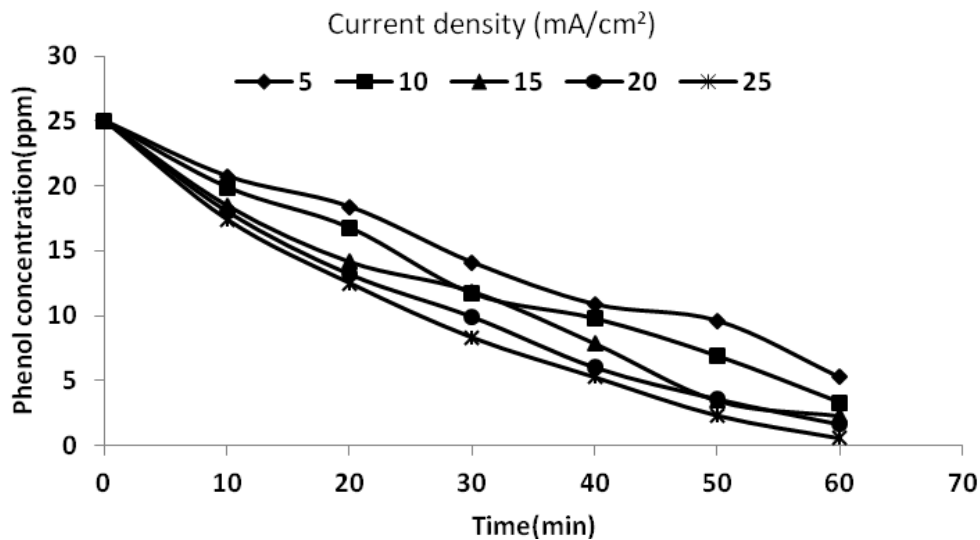


Figure 5. Effect of current density on phenol degradation during electro-oxidation process ($C_0=25\text{ppm}$, 3%NaCl, $T=25^\circ\text{C}$).

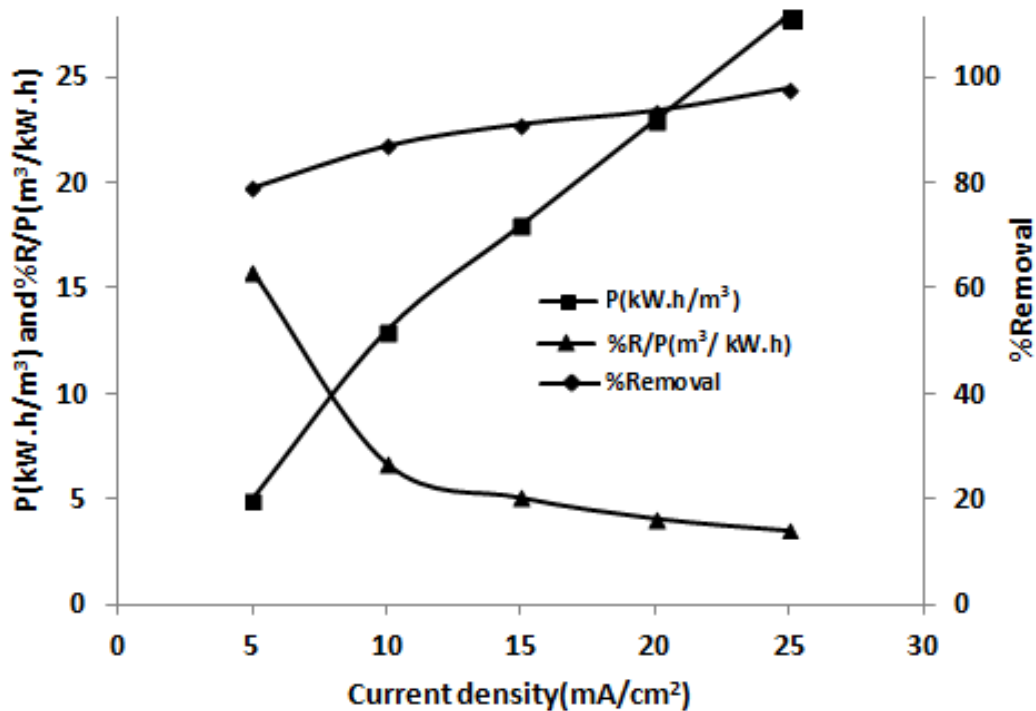


Figure 6. Effect of current density on power consumption and %removal.

These effects are both valuable for high pollutant removal. As seen in Fig.6, to compute the efficiency of the processes, power consumption was calculated. Commonly power consumption was expressed in kWh/m³ and given as:

$$\text{Power consumption (kW.h/m}^3\text{)} = \frac{I V t}{\text{vol}} \quad (4)$$

Where V = applied voltage (V), I = applied current (A), t = electrolysis time (h) and vol = solution volume (m³). From the results of electrooxidation of phenol, maximum phenol degradation of about 98% was acquired with an energy consumption about 27.5 kWh/m³. The ratio (R/P), that represents the ratio between the rate of phenol removal and the power consumed per m³ of the solution was used for optimizing the current density which approach the highest removal % per lowest amount of power. The experimental results showed that among these different current densities, 25 mA/cm² is the best current density where highest % phenol degraded and lower (R/P) ratio. These results indicate that the process favors the increase of current density up to the studied level. In addition, we have to consider the effect of increasing the current density on the production rate of Cl₂ due to the electrolysis of the NaCl electrolytic solution, which have indirect effect on the electrooxidation of phenol.

3.3. Effect of phenol concentration on the electrooxidation of phenol

Effect of phenol concentration from 10 to 100 mg/l on the removal efficiency has been shown in Fig.7. It can be detected that an increase in phenol concentration for same electrooxidation time and current density results in a decrease in removal efficiency. This can be ascribed to the fact that at a constant current density, a same number of ions passes to the solution at different phenol concentrations. Therefore, the formed amount of Cl₂ required for indirect electrooxidation of phenol and/or the potential required for direct oxidation of the phenol on surface of the PCGE anode will be sufficient only for certain amount of the phenol, above this limit the Cl₂ will be insufficient to degrade the greater number of phenol molecules at higher phenol concentrations. In addition, two more important parameters have to be considered; First; is the decrease in electrode activity due to higher concentrations of phenols, due to adsorption of phenol molecules to the PCGE surface, these results are consistent with the finding of Xavier[26], who studied the oxidation of phenol on Pt surface in presence of H₂SO₄ using cyclic voltametry, the authors found that, the cyclic peak current density increases by increasing the phenol concentration. They attributed this behavior to a decrease in electrode activity at higher concentrations of phenol, probably due to reduction in active sites on the electrode surface or to the formation of phenoxy radicals in big amounts at the electrode surface. Second; is the possibility of electropolymerization of phenol at the electrode surface and that will certainly block the active sites and reduce electrooxidation process to higher extent. This is also consistent with the finding of Singh [27], who found that for phenol concentrations lower than 5 mM the peak potential was practically unchanged with the phenol concentration, while Arslan [18] found that when the phenol concentration was increased to 0.1 M, the peak potential shifted to negative values both in acidic and in alkaline media. This behavior could be explained by a more availability of phenoxy radical associated to a higher phenol concentration, which favors the oxidation reactions that occur at less anodic potentials [28].

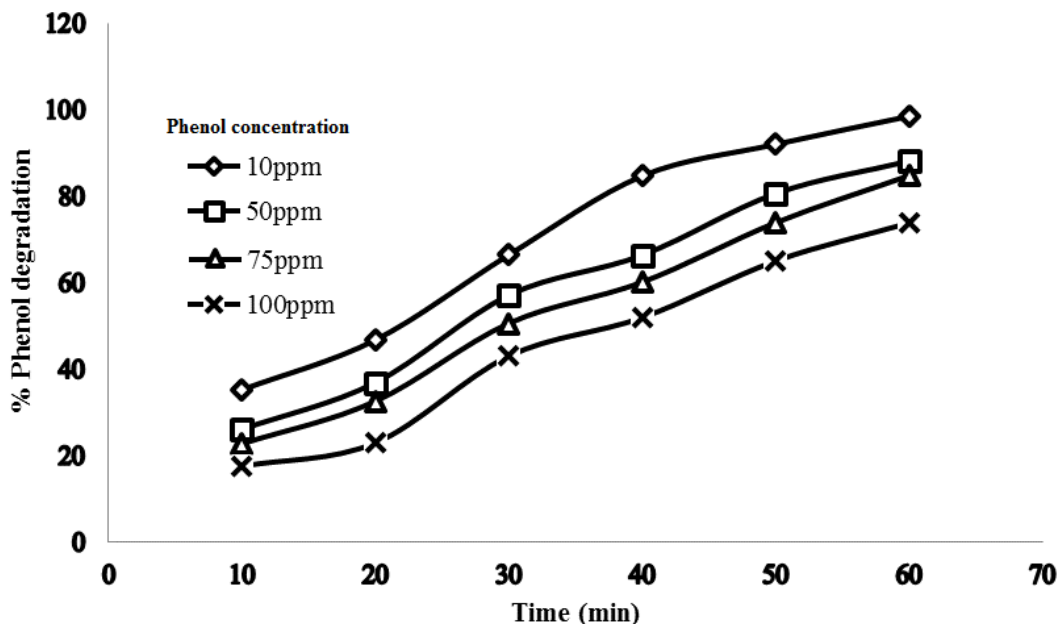


Figure 7. Effect of phenol concentration on efficiency of phenol degradation during electrooxidation process (current density=25mA/cm², 3%NaCl, T=25°C).

3.4. Effect of NaCl concentration on the electrooxidation of phenol

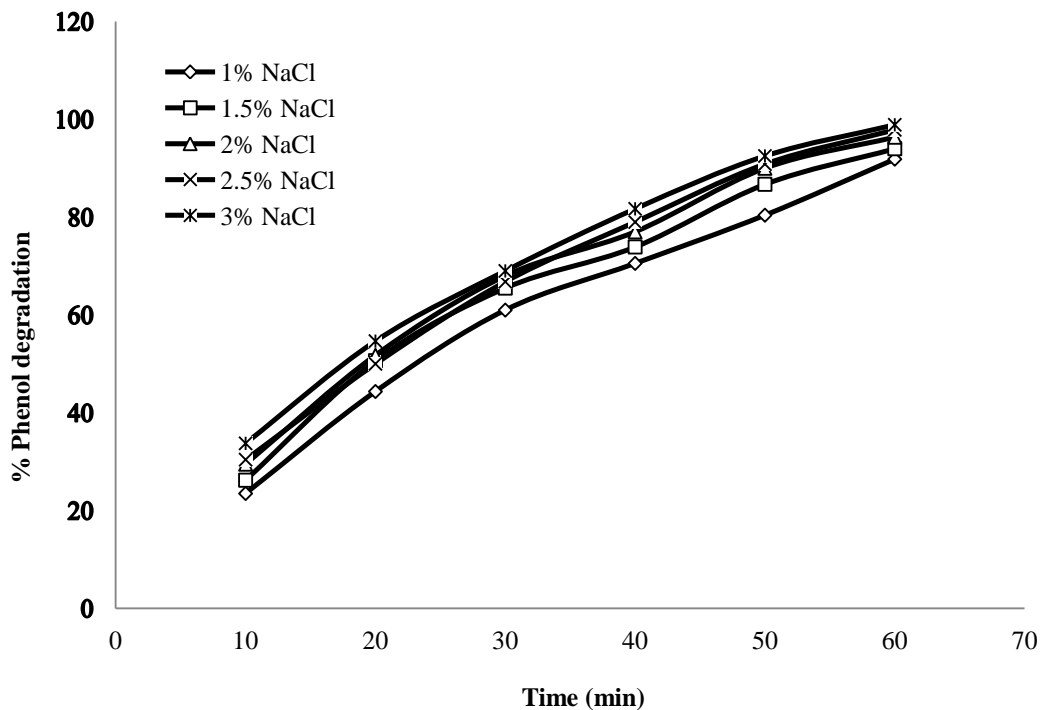


Figure 8. Effect of supporting electrolyte (NaCl) concentration on efficiency of phenol degradation during electrooxidation process (current density=25mA/cm², C₀=25ppm, T=25°C).

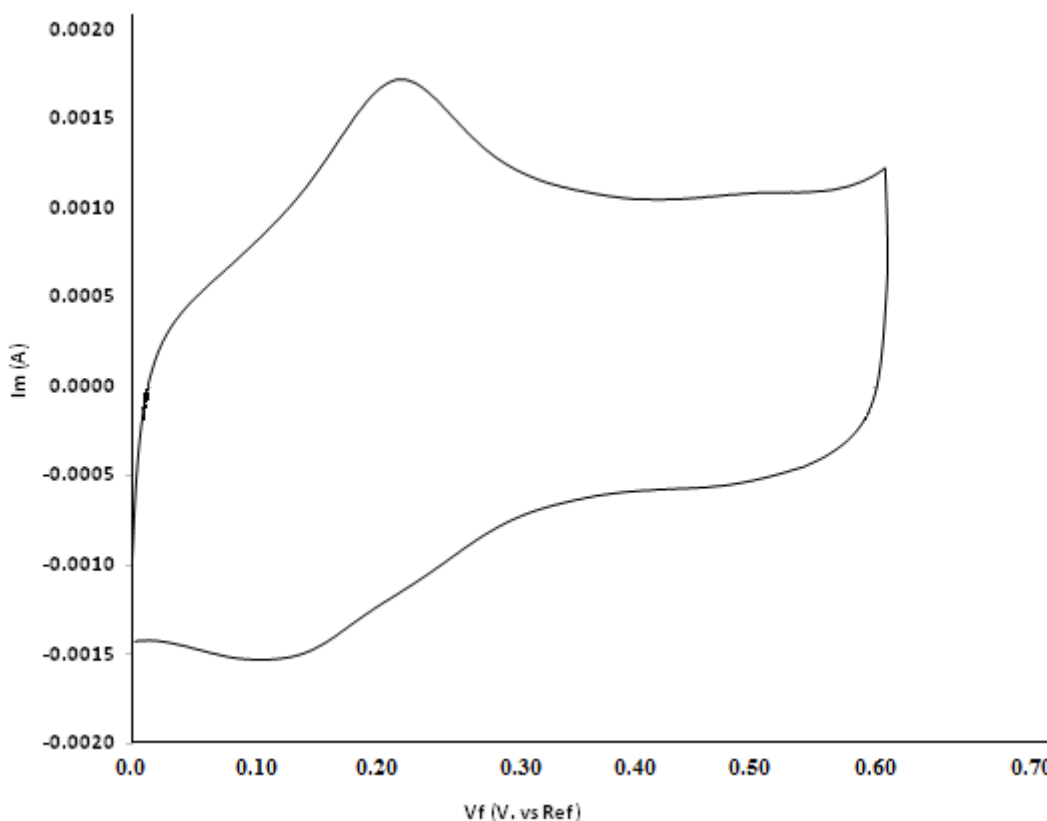
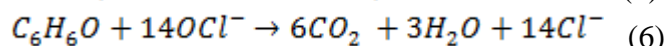
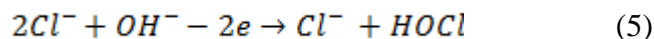


Figure 9. Cyclic Voltammetry examination of phenol degradation carried out at 50 mV/s scan rate, volt range from 0 to 0.6V, solution composition is 5ppm phenol and 3%NaCl.

Fig. 8 clearly shows that the phenol removal efficiency increases as the NaCl concentration of the feed solution increases from 0.5 to 3%. As shown the efficiency of phenol removal increased from 94% to 98% after 60 min of electrooxidation. The NaCl effectiveness on the electrooxidation of phenol might be ascribed to series of chemical reactions will take place in the solution bulk starting with the chloride ion oxidation that leads to the formation of chlorine, which in turn may react with either H₂O or OH⁻ to form HOCl which dissociates to OCl⁻ that can oxidize the phenol[29,30]. The main reactions involved can be summarized in following reactions:



Thus increasing the available amount of NaCl will increase the produced hypochlorite and thus increase the % phenol oxidized. In addition, increase in chloride anions will certainly increase the solution conductivity which in turn decreases the power consumption.

As shown in figure 9 and 10 the difference in the two figures is the presence of phenol, figure 9 represents the cyclic voltametry of a solution has both NaCl and phenol while figure 10 for a solution of NaCl only. As could be concluded from the two figures (9 and 10) a common peak at 0.0017 mA

and 0.205 V for both cases that means this peak belongs for the oxidation reaction of Cl^- according to equation 5 to produce HOCl which represents the main oxidizing agent for the phenol compound.

These results are consistent with the findings of Zhang and co-authors [31] reported that, hypochlorite production at the anode was found to be diffusion-controlled and rate-limiting. A 99% current efficiency was estimated for the indirect process, while that of the direct oxidation was 16%. And with the findings of Rajkumar[32] who recorded that a complete oxidation of phenol was carried out in a chloride-containing supporting electrolyte using Ti-supported $\text{TiO}_2\text{-RuO}_2\text{-IrO}_2$ ternary mixture .

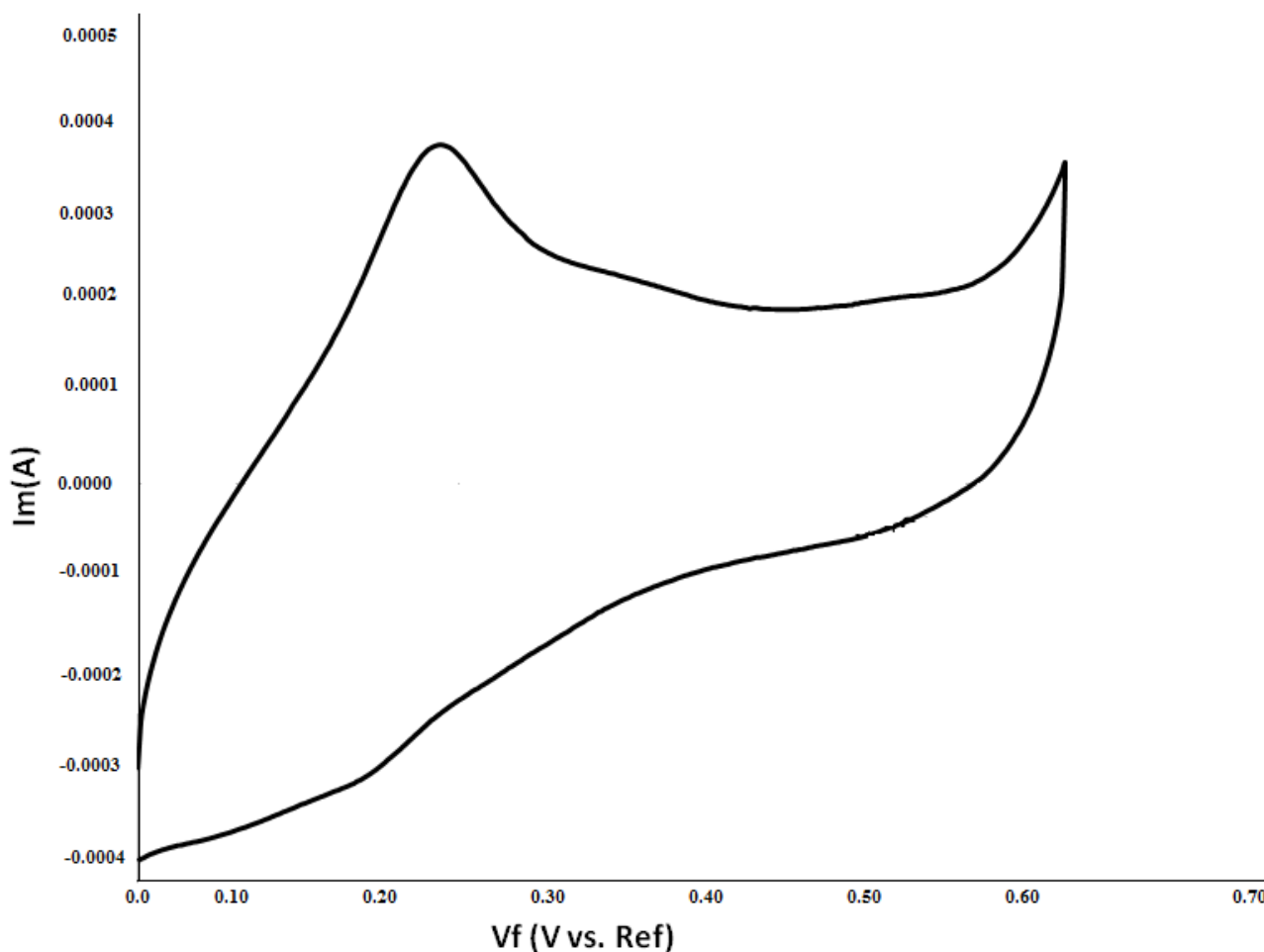


Figure 10. Cyclic Voltammetry examination of NaCl degradation carried out at 50 mV/s scan rate, volt range from 0 to 0.6V and solution contain 3%NaCl only.

3.5. Kinetics of phenol degradation

Fig.11 shows that the electrooxidation reaction kinetics data obtained for phenol degradation are well fitted by the first order rate equation in the form:

$$V_{sol} \ln(C_0/C) = kAt \tag{7}$$

Where V_{sol} is the solution volume, C_0 and C are the initial phenol concentration and its concentration at any time t , k is the mass transfer coefficient and A is the electrode area. For this

analysis the volumetric mass transfer coefficient ($K=kA$) was used. The mass transfer coefficient was calculated by plotting $\ln(C_0/C)$ vs t for different conditions of current density, phenol concentration and NaCl concentration.

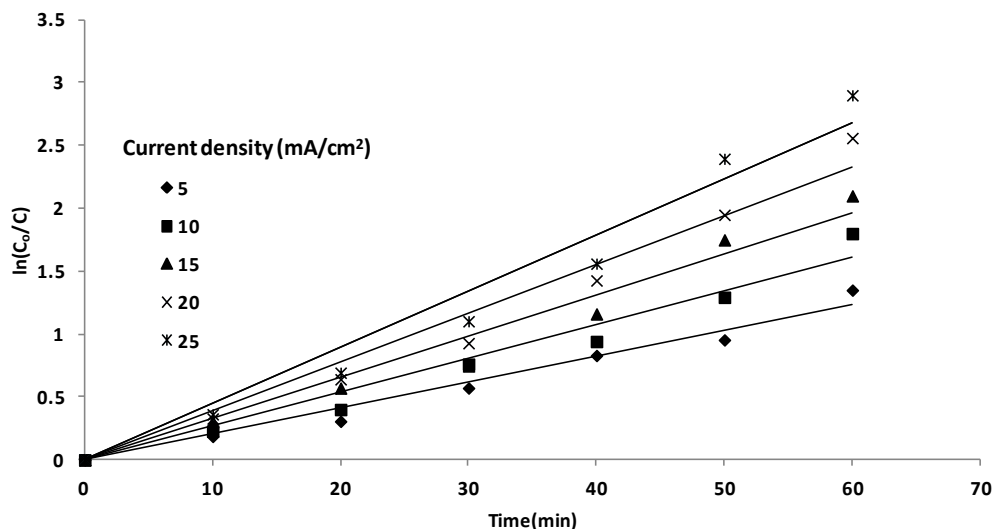


Figure 11. $\ln(C_0/C)$ vs. time at different current densities.

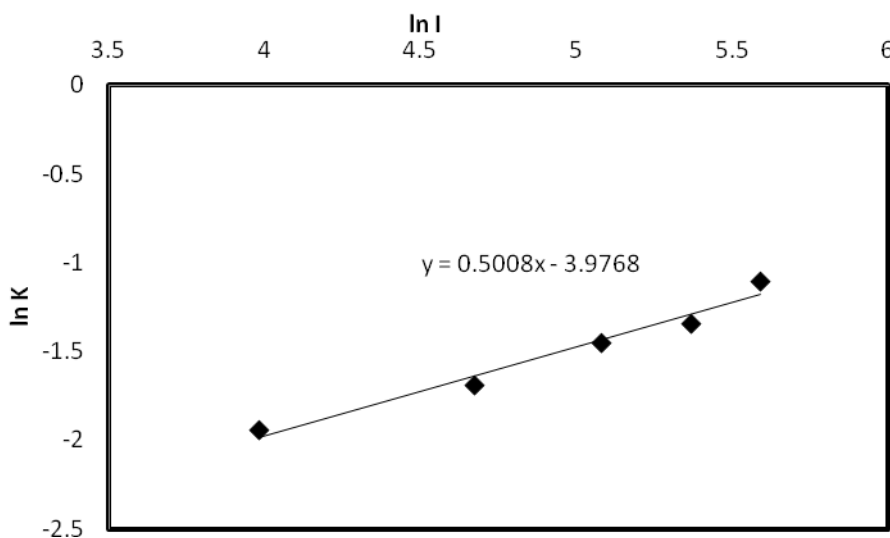


Figure 12. $\ln(K)$ vs $\ln(I)$.

From the slope of each line K was calculated as (slope= K/V_{sol}). Figure 11 shows an example for the effect of current density. The results as shown in figures 11 and 12 show that the calculated mass transfer coefficient increases by rising the current density. For modeling of the relation associating the mass transfer coefficients with current of electrooxidation a relation in the form:

$$K = \alpha I^\gamma \tag{7}$$

was considered. Fig.12 shows a relation between $\ln K$ versus $\ln I$ for finding out the values of α and γ for phenol degradation. The results show that a relation in the form that:

$$K = \alpha I^{0.5008} \tag{8}$$

on the same direction, correlations of the same type were obtained for the effect of both phenol and NaCl concentrations. As shown in figures 13 and 14 correlations of the forms:

$$K = \alpha_1 C_{Ph}^{0.42} \tag{9}$$

And

$$K = \alpha_2 C_{NaCl}^{0.42} \tag{10}$$

Were obtained.

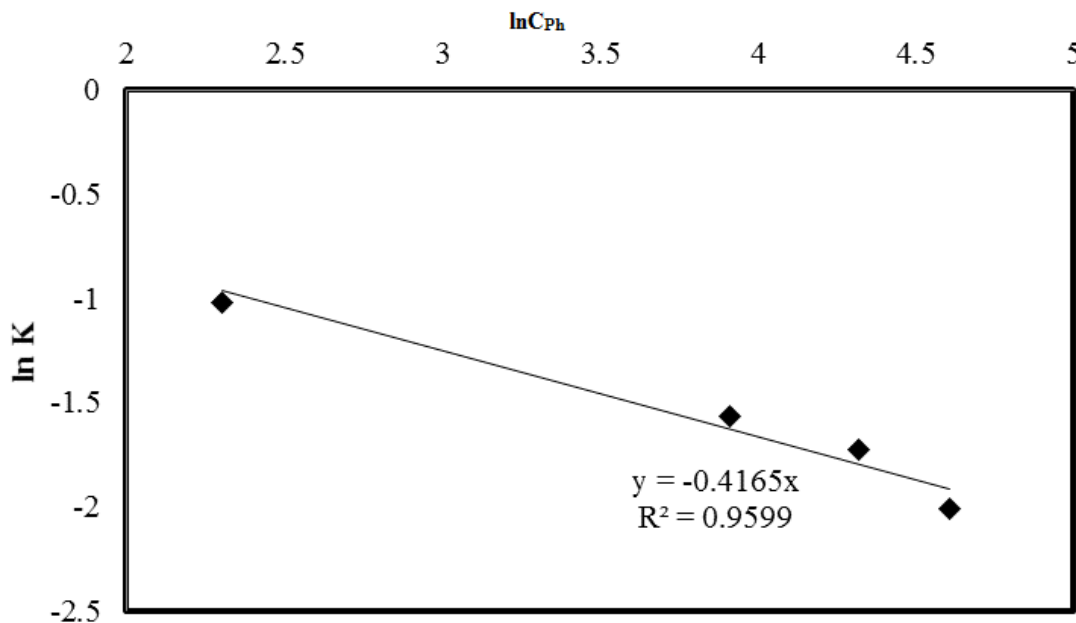


Figure 13. ln(K) vs ln(C_{Ph})

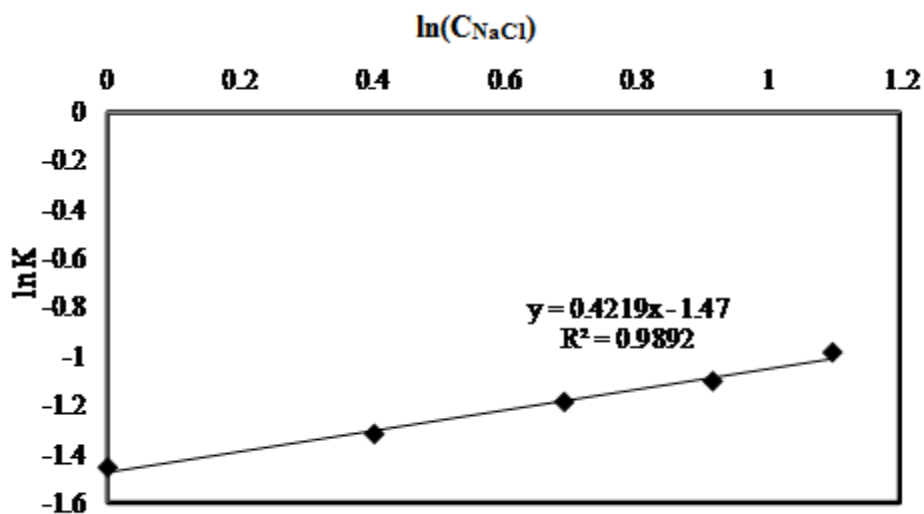


Figure 14. ln(k) vs ln(C_{NaCl}).

3.6. Comparison between PCGE and BG

For the comparison between the two electrodes, bare graphite (BG) and polyaniline coated graphite(PCGE), the % improvement was calculated as in equation 2. As shown in figure 15 the % removal has been increased by increasing the time for both electrodes, while % improvement increased to certain level up to 40 min, after that time the % improvement decreased, that means the efficiency of the electrooxidation process using PCGE decreases with time, that's might be attributed to the possible precipitation of phenol and/or its derivative on the PCGE surface which increase anode polarization and decrease its efficiency for further oxidation of phenol molecules. However the results show that an improvement of the process efficiency up to 35% can be achieved using the developed PCGE electrode.

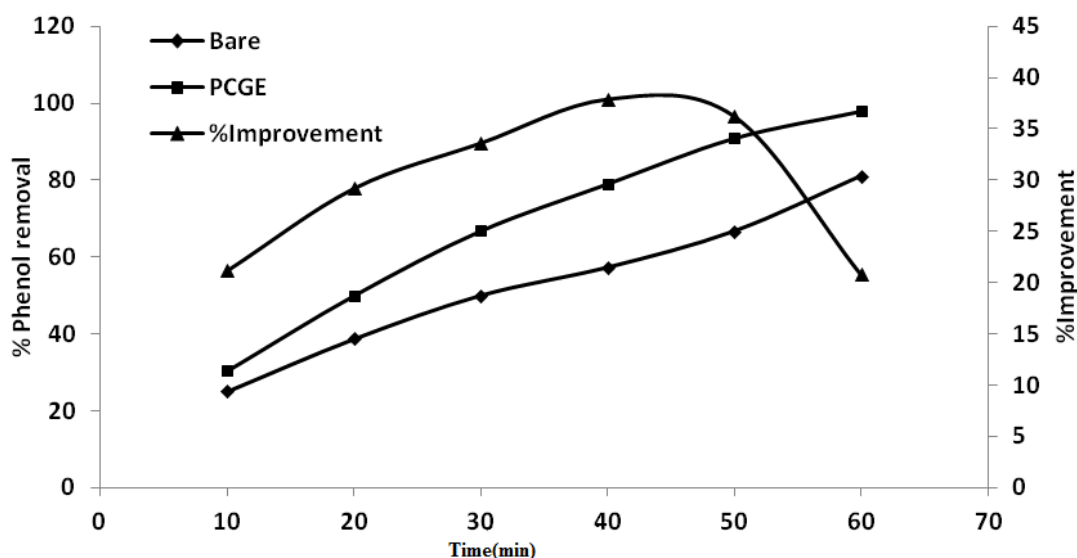


Figure 15. %Phenol removal for both BG and PCGE and % Improvement vs time at 25mA/cm² and 3%NaCl.

3.7. Comparison between the new electrode PCGE and different electrodes used by other authors

Table 1; shows the comparison of the results obtained using the new PCGE electrodes and other electrodes used by different researchers, the results shows that Boron doped diamond (BDD) and Ti/SnO₂ has the a higher removal efficiencies of 94% (COD removal) at 1000 A/m² and 100% removal at 500 A/m² compared to other electrodes respectively. However for the PCGE the efficiency was 98% at lower current density of 250 A/m².

Table 1. Comparison between PCGE and other electrodes

Electrode Type	Pollutant	Conditions	Efficiency	Reference
Granular graphite	Phenol	0.03-0.32 A/m ²	70% CE, 50%	33

Planar graphite	Phenol	10-100 A/m ²	24.6-63.5%, 17% COD,	34
Porous Graphite	Phenol	2.0 A	48% CE	35
Pt	Phenol	30 mA/cm ²	25% (1.5 h), EOI=0.13	36
PbO ₂	Phenol	E= 1.4-2.5 V	68-100%	37
BDD	Phenol solution	1000 A/m ²	94% COD	38
Ta/PbO ₂	Phenol	100-200 mA/cm ²	60 °C=80%	39
Ti/BDD	phenol	100 A/m ²	78.5% CE , 97% COD	40
Ti/IrO ₂	phenol	<50mA/cm ²	EOI=0.17, 71%	41
Ti/IrO ₂	phenol	50 mA/cm ²	80%	42
Ti/SnO ₂	phenol	50 mA/cm ²	100%	42
PCGE	phenol	25 mA/cm ²	98%	Present work

4. CONCLUSIONS

Phenol removal from synthetic aqueous solutions containing different concentrations of phenol up to 100 mg/l by electrooxidation using polyaniline coated graphite electrode PCGE has been investigated. From the study it can be concluded that electrooxidation process on PCGE is highly advantageous in the degradation of phenol from aqueous solution. It has been found that, the extent of degradation of phenol is a function of the applied current, electrolysis time, concentration of phenol and concentration of supporting electrolyte (NaCl). According to the results, an increase in current density and NaCl concentration can increase the efficiency of phenol removal. Conversely, increasing initial phenol concentration result in decreasing phenol removal by electrochemical oxidation. The optimum value of current density, allowing high removal rates (98%) of phenol removal was found to be 25 mA/cm². Based on the results of this study, a 35% improvement of the phenol removal efficiency by electrooxidation using PCGE electrodes was achieved. In addition 27.5 kWh/m³ was required for the treatment using the PCGE electrode.

ACKNOWLEDGEMENT

This project was funded by the National Plan for Science, Technology and Innovation (MAARIFAH)–King Abdulaziz City for Science and Technology–the Kingdom of Saudi Arabia–award number (12-ADV2760-03). The authors also, acknowledge with thanks Science and Technology Unit, King Abdulaziz University for technical support.

References

1. Y. Fang, Q. Jiang, M. Deng, Y. Tian, Q. Wen and M. Wang, *J. Electroanal. Chem.*, 755(15) (2015) 39.

2. C. Hui-Fang, D. Lin, G. Peng-Bo, Z. Bao and J.H.T. Luong, *J. Power Sources*, 283 (2015) 46.
3. L.Z. Pei, Z.Y. Cai, Y.K. Xie and D.G. Fu, *Measurement*, 53 (2014) 62.
4. M. Guerra-Balcázar, R.Ortega, F. Castaneda, L.G. Arriaga and J. Ledesma-Garcia, *Int. J. Electrochem. Sci.*, 6 (2011) 4667.
5. F. Yang, L. Ma, M. Gan, J. Zhang, J. Yan, H. Huang, L. Yu, Y. Li, C. Ge and H. Hu, *Synth. Met.*, 205 (2015) 23.
6. B. Rajender, G. Ramesh and S. Palaniappan, *Catalysis Commun.*, 43(5) (2014) 93.
7. K. Chung-Wen, K. Zheng-Yan, J. Jiin-Jiang, W. Tzi-Yi, C. Jing-Yuan and Z. Xian-Xun, *Int. J. Electrochem. Sci.*, 7 (2012) 4974.
8. Y.A. Alhamed, A.H. El-Shazly, A.A. Al-Zahrani and M.A. Daous, *Int. J. Electrochem. Sci.*, 11 (2016) 486.
9. A.H. El-Shazly and H.A. Al-Turaif, *Int. J. Electrochem. Sci.*, 7 (2012) 5388.
10. A.H. El-Shazly, A.A. Wazan and T.A. Radain, *Int. J. Electrochem. Sci.*, 7 (2012) 2416.
11. A.H. El-Shazly and H.A. Al-Turaif, *Int. J. Electrochem. Sci.*, 7 (2012) 211.
12. D.S. Patil, S.A. Pawar, S.K. Patil, P.P. Salavi, S.S. Kolekar, R.S. Devan, Y.R. Ma, J.H. Kim, J.C. Shin and P.S. Patil, *J. Alloys Compd.*, 646(15) (2015) 1089.
13. D.S. Patil, S.A. Pawar, R.S. Devan, Y.R. Ma, W.R. Ba, J.H. Kim and P.S. Patil, *Mater. Lett.*, 117 (2014) 248.
14. X. Ma, Y. Feng, Y. Li, Y. Han, G. Lu, H. Yang and D. Kong, *Chin. J. Catalys.*, (36)(7) (2015) 943.
15. F. Ficiocioglu and F. Kadirgan, *J. Electroanal. Chem.*, 451 (1998) 95.
16. F. Yang, L. Ma, M. Gan, J. Zhang, J. Yan, H. Huang, L. Yu, Y. Li, C. Ge and H. Hu, *Synth. Met.*, 205 (2015) 23.
17. Z.F. Guo, R.X. Ma and G.J. Li, *Chem. Eng. J.*, 19 (2006)55.
18. O. Gimeno, M. Carbajo, F.J. Beltrán and F.J. Rivas, *J. Hazard. Mater.*, B119 (2005) 99.
19. R. Kidak and N.H. Ince, *Ultrason. Sonochem.*, 13 (2006) 195.
20. B. Zkaya, *J. Hazard. Mater. B*, 129 (2006) 158.
21. A. Kapalka, G. Foti and Ch. Comninellis, *Electrochim. Acta*, 54 (2009) 2018.
22. Y. Cong and Z. Wu, *J. Phys. Chem. C*, 111 (2007) 3442.
23. X. Zhu, M. Tong, S. Shi, H. Zhao and J. Ni, *Environ. Sci. Technol.*, 42 (2008) 4914.
24. M. Trchová and J. Stejskal, *Pure Appl. Chem.*, 83(10)(2011)1803.
25. C.W. Tobias, M. Eisenberg and C.R. Wilke, *Electrochem. Ionic Cryst.*, (12)(99) (1952) 359c.
26. J.L.N. Xavier, E. Ortega, J.Z. Ferreira, A.M. Bernardes and V. Pérez-Herra, *Int. J. Electrochem. Sci.*, 6 (2011) 622.
27. R.N. Singh, D. Mishra and Anindita, *Int. J. Electrochem. Sci.*, 4 (2009) 1638.
28. G. Arslan, B. Yazici and M. Erbil, *J. Hazard. Mater.*, 124 (2005) 37.
29. F. Bonfatti, A. Battisti, S. Ferro, G. Lodi and S. Osti, *Electrochim. Acta*, 46 (2000) 305.
30. Ch. Comninellis and A. Nerini, *J. Appl. Electrochem.*, 25 (1995) 23.
31. X.M. Zhan, J.L. Wang, X.H. Wen and Y. Qian, *Environ. Technol.*, 22 (2001) 1105.
32. D. Rajkumar, J.G. Kim and K. Palanivelu, *Chem. Eng. Technol.*, 28 (2005) 98.
33. Y.M. Awad and N.S. Abuzaid, *J. Environ. Sci. Health A*, 32 (1997) 1393.
34. N. Kannan, S.N. Sivadurai, J.L. Berchmans and R. Vijayavalli, *J. Environ. Sci. Health*, A30 (1995) 2185.
35. Y.M. Awad and N.S. Abuzaid, *Sep. Purif. Technol.*, 18 (2000) 227.
36. Ch. Comninellis and C. Pulgarin, *J. Appl. Electrochem.*, 21 (1991) 703.
37. B. Idbelkas and D. Takky, *Ann. Chim. Sci. Mat.*, 26 (2001) 33.
38. J.J. Carey, J.C.S. Christ and S.N. Lowery, *US Pat.*, 5 399 247, (1995).
39. I. Troster, M. Fryda, D. Herrmann, L. Schafer, W. Haenni, A. Perret, M. Blaschke, A. Kraft and M. Stadelmann, *Diamond Relat. Mater.*, 11 (2002) 640.
40. X. Chen, G. Chen, F. Gao and P.L. Yue, *Environ. Sci. Technol.*, 37 (2003) 5021.
41. Ch. Comninellis, *Trans. Ichem E. B*, 70 (1992) 219.

42. Ch. Comninellis, *Electrochim. Acta*, 39 (1994) 1857.

© 2017 The Authors. Published by ESG (www.electrochemsci.org). This article is an open access article distributed under the terms and conditions of the Creative Commons Attribution license (<http://creativecommons.org/licenses/by/4.0/>).